Vol. 175: 261–276, 1998 | MARINE ECOLOGY PROGRESS SERIES
Mar Ecol Prog Ser | Published December 17

Seasonal carbon and nutrient mineralization in a high-Arctic coastal marine sediment, Young Sound, Northeast Greenland

Søren Rysgaard[1,*], Bo Thamdrup[2], Nils Risgaard-Petersen[3], Henrik Fossing[1], Peter Berg[4], Peter Bondo Christensen[1], Tage Dalsgaard[1]

[1]Dept. Lake and Estuarine Ecology, National Environmental Research Institute, Vejlsøvej 25, DK-8600 Silkeborg, Denmark
[2]Max Planck Institute for Marine Microbiology, Celsiusstr. 1, D-28359 Bremen, Germany
[3]Institute for Biological Sciences, Department of Microbial Ecology, University of Aarhus, Ny Munkegade, DK-8000 Århus C, Denmark
[4]Dept. Environmental Sciences, Clark Hall, University of Virginia, Charlottesville, Virginia 22903, USA

ABSTRACT: A comprehensive investigation of carbon and nutrient cycling in Arctic marine sediments is presented. The high-Arctic fjord Young Sound in Northeast Greenland was chosen as study site. The fjord was covered by sea ice for approximately 10 mo during 1996. Despite highly fluctuating seasonal air temperatures, the bottom water temperature remained almost constant at −1.2 to −1.8°C throughout the year. When sea ice broke in mid-July, benthic mineralization was immediately stimulated by a significant peak in sedimentation of organic material. Due to rapid mineralization of the easily degradable fraction of the settling organic material, respiration rates returned to their basic lower level within 1 mo and remained low for the rest of the season. Benthic mineralization rates in the Young Sound sediment are comparable with rates from much warmer locations, suggesting that benthic mineralization in this high-Arctic coastal sediment was regulated by the availability of organic matter and not by temperature. Rate measurements covered oxygen respiration, denitrification, manganese, iron, and sulfate reduction as well as DIC and nutrient flux from the sediment. In response to enhanced mineralization following sea ice break-up, sediment water fluxes of O_2, DIC, $NO_3^- + NO_2^-$, NH_4^+, urea, PO_4^{3-}, and Si increased and rapidly recycled nutrients to the water column, indicating an efficient benthic-pelagic coupling in Young Sound. Sediment porewater concentrations of O_2 were affected by the input of organic matter, leading to higher O_2 consumption rates near the sediment surface during summer. In contrast, no seasonal alterations in concentration profiles of DIC, NH_4^+, $NO_3^- + NO_2^-$, Mn^{2+}, Fe^{2+} and SO_4^{2-} were observed. Furthermore, depth distributions of e^--acceptors (O_2, NO_3^-, Fe(III) and SO_4^{2-}) and reduction rate measurements supported the classical orderly progression from O_2 respiration to NO_3^- reduction followed by bacterial iron reduction and finally sulfate reduction. On an annual scale, O_2 respiration accounted for 38% of total oxidation of organic carbon, denitrification, 4%; iron reduction, 25%; and sulfate reduction, 33%. Rates of carbon oxidation by manganese reduction were insignificant (<1%) and the fraction of refractory carbon buried was approximately equal to the amount of carbon being mineralized in Young Sound.

KEY WORDS: Sediments · Fluxes · Denitrification · Manganese · Iron · Sulfate reduction · Porewater · Nutrients · Burial

INTRODUCTION

The waters north of the Arctic Polar Circle are characterized by a strong contrast between summer and winter. In these high latitudes the amount of particulate organic matter originating from primary production is strongly influenced by large seasonal variations in insolation. Furthermore, the presence or absence of sea ice is an important factor controlling the availability of light for primary producers. Under complete ice cover, sedimentation is very low, whereas maximum sedimentation is found at the sea ice margin when sea

*E-mail: sr@dmu.dk

ice breaks during the short summer thaw (Atkinson & Wacasey 1987, Hebbeln & Wefer 1991). Thus, in Arctic areas seasonal variations in sea ice cover limit the sedimentation to the short summer period, and the input of organic matter to the sediment surface is often characterized by a strong pulse following the spring bloom in the water column.

Observations from temperate coastal marine areas with large seasonal variation in bottom water temperature have revealed that low temperatures tend to decrease microbial activity (Pomeroy & Deibel 1986, Shiah 1994, Thamdrup et al. 1998), leading to the suggestion that microbial community respiration in general is low in cold waters (Pomeroy & Deibel 1986). However, recent investigations have pointed out that both the efficiency and rates of benthic mineralization in permanently cold sediments (Nedwell et al. 1993, Rysgaard et al. 1996, Glud et al. 1998) can be as high as those obtained in temperate and tropical sediments (Pamatmat 1973, Rasmussen & Jørgensen 1992, Tahey et al. 1994, Thamdrup et al. 1996).

Experimental studies have shown that increased additions of organic matter enhance bacterial activity (Kelly & Nixon 1984, Caffrey et al. 1993). However, in temperate areas it is often difficult to separate the effect of increased organic sedimentation from a simultaneous *in situ* temperature increase. Furthermore, the timing of organic matter input to the sediment following a bloom is difficult to predict, which creates the need for a long and intensive sampling period. However, Arctic marine ecosystems with extended sea ice cover may be ideal for such *in situ* sedimentation experiments because bottom water temperatures do not change over the seasons and the spring bloom associated with the ice break-up can be predicted within a margin of few days (Wadhams 1981).

The main focus of this paper is to quantify seasonal benthic mineralization within a high-Arctic marine ecosystem with permanently cold bottom water (<–1°C) and thereby increase our knowledge of benthic bacterial activity at low temperatures. We describe how, where, and when settling organic matter is degraded by microbes within the sediment during a 10 mo period of sea ice cover followed by an increased input of organic matter to the sediment during the 2 mo summer thaw. We also discuss the relative importance of O_2, NO_3^-, Mn, Fe and SO_4^{2-} as e^--acceptors in the oxidation of organic matter within the sediment of an Arctic fjord.

Since oxidation of organic matter in sediments results in release of dissolved inorganic carbon (DIC) and nutrients (N, P, Si) which eventually become available to primary producers, the study also includes a discussion of annual sediment-water fluxes. Furthermore, the fraction of organic matter that is not oxidized within the sediment but becomes buried and preserved will be addressed. Finally, we construct an annual carbon budget, covering sedimentation, mineralization, and burial at this 36 m location in Young Sound, Northeast Greenland.

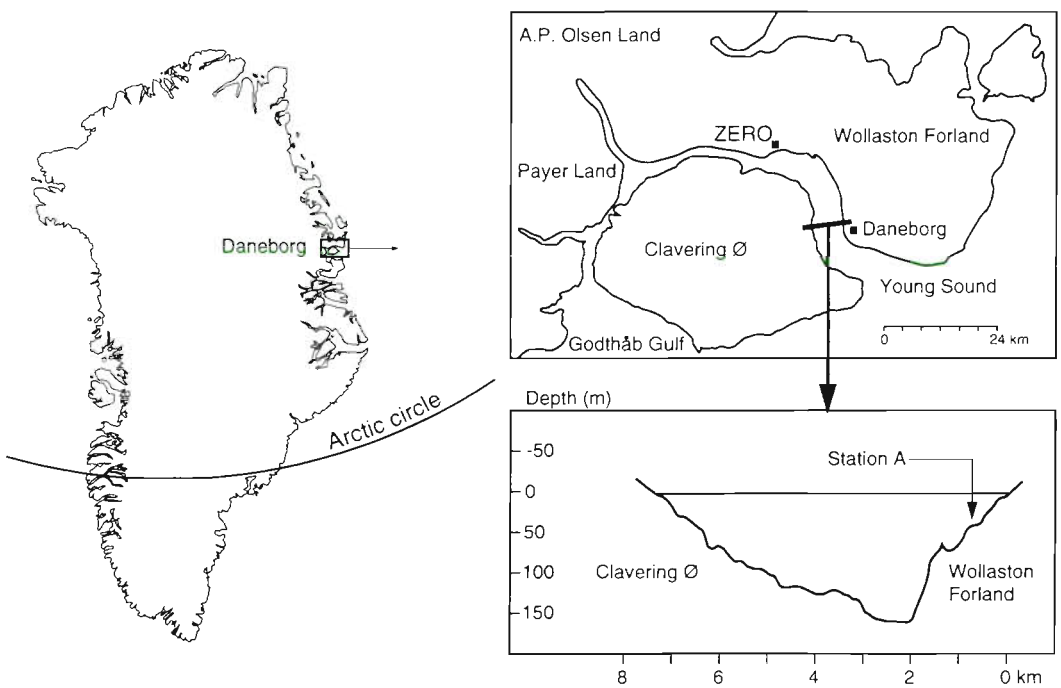

Fig. 1. Location of sampling station in Young Sound near Daneborg, Northeast Greenland. Water depth: 36 m. (ZERO = Zackenberg Ecological Research Operations)

MATERIAL AND METHODS

Study site. The investigation was carried out in the Young Sound fjord in Northeast Greenland, at a location off Daneborg, 25 km SSE of the Zackenberg Ecological Research Station, ZERO (Fig. 1). Intensive sampling took place from June through August 1996 and during February 1997 at a water depth of 36 m at 74° 18.58' N, 20° 15.04' W (Stn A).

Young Sound was covered by sea ice for approximately 10 mo in the period 1996-1997 and, despite air temperatures above 0°C during summer, the bottom water temperature at the sampling station remained <-1°C (Fig. 2). The hydrographic conditions of the Sound are described in further detail in Rysgaard et al. (1999). In short, a stable pycnocline at 15 m depth was maintained by a large melt water input from land and sea ice, and from the tidally stimulated inflow of cold, highly saline polar water from the East Greenland Current. The water column structure caused the pelagic primary production to peak relatively deep in the water column (~15 m) due to nutrient limitation in surface waters (Rysgaard et al. 1999).

Sediment and water sampling. During February, June, and July sampling of bottom water and sediment took place through a hole in the sea ice using a tripod mounted with a 5 l Niskin water sampler or a sediment sampler (modified Kajak sampler). During ice-free conditions in August, the equipment was handled from a boat. Sediment was cored in 30 × 5.3 cm Plexiglas tubes that sampled 22 cm^2 of the sea bottom. Only undisturbed sediment cores with clear overlying water were used. In total, 9 sampling campaigns were carried out to describe the annual variation of sediment mineralization.

All sediment cores were immediately placed in an insulated box and brought back to the laboratory within 1 to 2 h. In the laboratory, a small Teflon-coated magnet (0.5 × 3 cm) was placed 5 cm above the sediment surface and the core was submerged into a tank with *in situ* bottom water and kept in darkness at *in situ* temperature and air saturation. Mixing of the water column was provided by rotating (60 rpm) the Teflon-coated magnets. All cores were pre-incubated for 1 d before further processing to minimize disturbances from coring and transport.

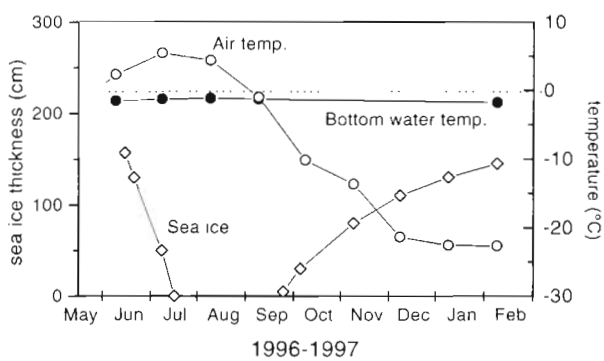

Fig. 2. Air temperature, bottom water temperature, and sea ice thickness at the sampling station during the investigation period

Sediment characteristics, sedimentation and burial. Porosity was calculated in 1 cm fractions of 4 sediment cores from density and water content measured as weight loss after drying at 105°C for 24 h.

Organic carbon and nitrogen content was determined on 4 replicate sediment cores sliced into 3 to 10 mm fractions and frozen for later analysis. Prior to analysis each fraction was treated with HCl, freeze dried, homogenized and weighed into sample boats. Analyses were performed on a C/N elemental analyzer (RoboPrep-C/N, Europa Scientific, UK).

Two measurements of sedimentation rate were made during the study; one during sea ice cover in June and one during the open-water period in late July. Sediment traps were placed in duplicates at 7, 14, 18, 27 and 35 m above the sediment surface for 7 d. The traps (Plexiglas tubes, 45 cm long with an i.d. of 8 cm) were suspended to remain vertical and in pairs perpendicular to the current. The trapped material was filtered through pre-combusted and weighed Whatman GF/F glass-fiber filters and frozen for later analysis. The filters were dried, weighed and combusted on the elemental analyzer in line with a mass spectrometer (TracerMass, Europa Scientific) in order to measure the carbon and nitrogen content of the settling material.

Sediment burial rate was determined from a core sectioned into 0.5 to 1 cm fractions down to 12 cm and frozen for later ^{210}Pb and ^{137}Cs analysis. The sediment fractions were freeze dried and homogenized prior to analysis. The non-destructive technique described by Joshi (1987) was used for analyzing ^{210}Pb and ^{137}Cs in the sediment sections. Sediment burial was calculated according to Christensen (1982). The carbon and nitrogen burial rates were calculated from the ^{210}Pb data, density, dry weight and average carbon and nitrogen content below 10 cm.

Sediment porewater chemistry. On each sampling occasion, 6 to 10 vertical concentration profiles of O_2 were measured with a Clark-type O_2 microelectrode (Revsbech 1989) at 200 µm intervals in 3 sediment cores. Measurements were performed at *in situ* temperature with an overlying water column of 2 cm aerated by a flow of atmospheric air to ensure sufficient stirring while measuring.

On 1 sampling occasion, 4 vertical concentration profiles of NO_3^- + NO_2^- were measured on 4 sediment cores with the newly developed NO_3^- microsensor

(Larsen et al. 1997). These profiles were measured after 24 h of pre-incubation at 3°C, which was the lowest temperature allowing successful operation of the sensor. All measurements were made at 1 mm intervals.

Porewater extractions for measurement of vertical concentration profiles of NH_4^+, DIC, Fe^{2+}, Mn^{2+}, H_2S, and SO_4^{2-} were performed with a pneumatic squeezer (modified after Reeburgh 1967). For NH_4^+ and DIC, 3 replicate cores were used. The cores were sectioned in 3 to 10 mm slices and porewater was extracted through Whatman GF/F glass-fiber filters using a pressure of 3 to 5 bar. The porewater samples for NH_4^+ determination were immediately frozen (–18°C) in 5 ml plastic vials. Porewater for DIC determination was sampled into 1.8 ml glass vials capped with butyl rubber septa, leaving no headspace, and preserved with 50 µl $HgCl_2$ (5% w/v) until later analysis. Sectioning and squeezing for Mn^{2+}, Fe^{2+}, H_2S and SO_4^{2-} took place in an N_2-filled glove bag to avoid oxidation of the compounds. Two cores were used for sampling for each of these parameters. Porewater was pressed through 0.45 µm cellulose acetate filters, and acidified with HCl to pH 2 (Mn^{2+} and Fe^{2+}) or fixed with Zn acetate (H_2S and SO_4^{2-}; 0.5% final conc.) and frozen until later analysis.

Concentrations of NH_4^+ and DIC were measured on 100 µl samples using the small-volume flow injection technique described by Hall & Aller (1992). Dissolved Fe^{2+} in porewater samples was determined by colorimetry with a Ferrozine solution without reducing agent (Stookey 1970). Dissolved Mn^{2+} was analyzed by flame atomic absorption spectroscopy. Sulfate was determined by non-suppressed anion chromatography, and H_2S was quantified by the methylene-blue technique (Cline 1969).

Sediment solid-phase chemistry. The depth distributions of manganese, iron, and sulfur species were determined on sediment collected in mid-July. For manganese and iron, samples of the sediment used in the bag incubations (see below) were collected and frozen under N_2 immediately after sectioning. Manganese was extracted with dithionite-citrate-acetic acid (DCA, pH 4.8; Lord 1980) while iron phases were quantified with a combination of acidic ammonium oxalate extractions of fresh and dried sediment (Thamdrup & Canfield 1996). This procedure separately measures poorly crystalline Fe(III) and particulate Fe(II) from phases such as FeS and $FeCO_3$, but not from pyrite.

Extracts of 10 ml were used with approximately 150 mg wet or 50 mg dry sediment. Extraction times were 1 h for DCA and 4 h for oxalate extractions (Canfield et al. 1993a, Thamdrup et al. 1994). Total extractable iron and Fe(II) were determined with Ferrozine (Thamdrup & Canfield 1996). Manganese was determined in the DCA extracts by flame atomic absorption spectroscopy.

Reduced sulfur was measured in preserved sediment from the sulfate reduction measurements (see below). Three cores were analyzed. Acid-volatile sulfide (AVS = FeS + H_2S) and chromium-reducible sulfur (CRS = FeS_2 + S^0) were determined after a 2-step distillation with cold 2 N HCl and boiling 0.5 M Cr^{2+} solution, respectively (Fossing & Jørgensen 1989).

Sediment-water fluxes. Exchange of O_2, DIC, NO_3^- + NO_2^-, NH_4^+, urea, PO_4^{3-}, and Si between the water column and sediment was measured on 6 intact equilibrated cores 24 h after sampling. The sediment height was adjusted to give sediment and water columns of ~12 and ~20 cm, respectively. As in the pre-incubation period, the water column was continuously stirred during the flux-rate experiments. The sediment cores were incubated in darkness at *in situ* temperature.

Flux measurements were initiated by closing the cores with a floating gas-tight lid (5.2 cm in diameter). To prevent gas exchange between water and the ambient atmosphere the lids were carefully removed only when water samples were collected. During incubation (24 to 48 h) changes in O_2 concentration in the water column never exceeded 20% of the initial O_2 concentration and water samples were collected 4 to 5 times within that period in order to verify a linear change in concentration over time.

The water samples were analyzed for O_2 concentration by Winkler titration within 12 h of sampling, and filtered (Whatman GF/F glass-fiber) water samples were immediately frozen (–18°) for later nutrient analysis. Water samples for DIC concentration determination were preserved in glass vials (Exetainer®, Labco, High Wycombe, UK) with 50 µl $HgCl_2$ (5% w/v). DIC concentrations were measured on a CO_2 analyzer (Coulometer CM5012, UIC Inc., Joliet, IL, USA). Concentrations of NO_3^- + NO_2^- were determined on a flow injection analyzer (Alpkem FS3000, Perstorp Analytical Environmental Inc., Oregon, USA) using the method described by Grasshoff et al. (1983). Ammonium concentrations were determined using the method of Bower & Holm-Hansen (1980). Urea concentrations were analyzed using the diacetylmonoxime method as described by Price & Harrison (1987). Phosphate and Si concentrations were determined by standard colorimetric methods as described by Grasshoff et al. (1983).

Sediment denitrification rates. The rate of denitrification was determined using the isotope pairing technique (Nielsen 1992) as described by Risgaard-Petersen & Rysgaard (1995) and Rysgaard et al. (1995). In short, $^{15}NO_3^-$ was added to the overlying water (30 to 50 µM final conc.) to initiate incubation and cores were closed with rubber stoppers leaving no headspace. A total of 6 sediment cores were incubated and the sediment cores were processed at different time intervals during the 24 to 48 h incubation period.

After incubation, subsamples of the water column and sediment were collected for analysis of the ^{15}N labelling of N_2 and NO_3^-. The samples for the ^{15}N abundance in NO_3^- were frozen (-18°C) until later analysis and samples for ^{15}N-N_2 analysis were preserved in glass vials (Exetainer®, Labco) containing 2% (vol) of a $ZnCl_2$ solution (50% w/v).

The abundance and concentration of $^{14}N^{15}N$ and $^{15}N^{15}N$ were analysed on a gas chromatograph coupled to a triple-collector isotopic ratio mass spectrometer (RoboPrep-G$^+$ in line with TracerMass, Europa Scientific) as described by Risgaard-Petersen & Rysgaard (1995). The ^{15}N isotopic distribution in the NO_3^- pool was likewise analyzed by mass spectrometry after reduction of NO_3^- to N_2 using a denitrifying bacterial culture (Risgaard-Petersen et al. 1993).

Sulfate reduction rates. Sulfate reduction rates were determined in intact sediment cores by the $^{35}SO_4^{2-}$ tracer method (Jørgensen 1978). Two or three cores of 26 mm i.d. were injected with 5 µl portions of carrier-free $^{35}SO_4^{2-}$ (80 kBq µl^{-1}; Risø Isotope Laboratory, Denmark) at 1 cm intervals through silicone-sealed ports from the sediment surface and down to 15 cm depth, and the cores were incubated at *in situ* temperature in the dark. After 24 h, the cores were sliced into 1 cm sections which were transferred immediately to plastic centrifuge tubes containing 10 ml 20% ZnAc, mixed, and stored frozen (-18°C) until analysis. The concentration of SO_4^{2-} was determined in each sediment fraction by unsuppressed anion chromatography using a Waters 510 HPLC pump, Waters WISP 712 autosampler (100 µl injection volume), Waters IC-Pak anion exchange column (50 × 4.6 mm), and a Waters 430 conductivity detector. Rates of sulfate reduction were measured and calculated as described in Fossing & Jørgensen (1989).

Total carbon and nitrogen mineralization rates. The depth distribution of carbon and nitrogen mineralization rates and pathways was determined in July-August 1996. Sediment from the upper 10 cm of 16 cores (352 cm^2 in total) was incubated as described by Canfield et al. (1993a) in Würgler bags, i.e. gas-tight laminated plastic bags (Hansen 1992, Kruse 1993). Within 4 h of retrieval, the cores were sectioned into eight depth intervals in an N_2-filled glove bag. Parallel intervals from different sediment cores were mixed in the incubation bags which were subsequently closed to eliminate any headspace and incubated for 15 d in a larger N_2-filled bag at *in situ* temperature. To minimize heating during handling in the glove bag at room temperature (~8°C) the sediment was kept on ice. Porewater was obtained on 5 subsequent occasions by pneumatic squeezing of subsamples from the bags through 0.45 µm cellulose-acetate filters in the N_2-filled glove bag. Samples for DIC were analyzed immediately while those for NH_4^+ were frozen. Analytical techniques were the same as described above. Total organic carbon and nitrogen mineralization rates were calculated from the linear increase in DIC and NH_4^+ concentrations over time.

Pathways of carbon mineralization. The contributions of manganese, iron, and sulfate reduction to carbon mineralization rates were determined from the bag incubations according to Thamdrup & Canfield (1996). In short, sulfate reduction rates in the bags were determined twice during the experiment from 24 h $^{35}SO_4^{2-}$ tracer incubations using the same technique and analysis as described above. Assuming a reaction stoichiometry of SO_4^{2-} to organic C of 1:2 (i.e. $SO_4^{2-} + 2CH_2O + 2H^+ \rightarrow 2CO_2 + H_2S + 2H_2O$), the sulfate-independent carbon oxidation was calculated by subtraction of sulfate-dependent carbon oxidation from total carbon oxidation (DIC accumulation) rates. In the sediment from below the O_2/NO_3^--containing surface layer, the excess carbon oxidation (i.e. carbon oxidation not caused by sulfate reduction) was assigned to bacterial reduction of either iron or manganese based on the depth distribution of oxidized and reduced iron and manganese in the solid phase (see above), and on the accumulation rates of Mn^{2+} and Fe^{2+} in the porewater during the incubation. Porewater concentrations of Mn^{2+} and Fe^{2+} from the incubations were determined as described above.

RESULTS

Sedimentation

The sediment traps collected the same amount of settling material at all depths and, therefore, resuspension was not evident (data not shown). Thus, sedimentation rates were calculated as the mean of the 5 depths. The rate of sedimentation during ice cover in June was 1.6 g dw m^{-2} d^{-1}. When sea ice broke in late July, the sedimentation rate increased to 2.5 g dw m^{-2} d^{-1} (Table 1). The rates correspond to a sedimentation of organic carbon and nitrogen of 17.3 and 1.4 mmol m^{-2} d^{-1}, respectively, during sea ice cover and 32.8 and 3.4 mmol m^{-2} d^{-1} during the open-water period in late July. Standard error of the mean sedimentation rates was <12%.

Solid-phase and porewater chemistry

The sea floor at the sampling station consisted of silty and cohesive/clayey sediment with a relatively high content of dropstones (diameter > 1 cm, 12.8 vol %) in the upper 10 cm (± 2.5 SE, n=10; sampled area 10 × 0.04 m^2). The porosity gradually decreased from 0.78

Table 1. Annual rates of sedimentation, burial, fluxes and processes from the 36 m station in Young Sound, NE Greenland

Sedimentation	
+ sea ice, mid June (g dw m^{-2} d^{-1})	1.6
– sea ice, late July (g dw m^{-2} d^{-1})	2.5
Total annual C and N flux[a] (mmol m^{-2} yr^{-1})	4405 carbon: 401 nitrogen
Burial	
Sediment growth rate (cm yr^{-1})	0.23
Sediment C and N burial (mmol m^{-2} yr^{-1})	2110 carbon: 205 nitrogen
Fluxes (mmol m^{-2} yr^{-1})	
O_2 consumption	2350
CO_2 production	2295
NO_3^- production	30
NH_4^+ production	33
Urea-N production	10
PO_4^{3-} production	13
Si production	443
Processes (mmol m^{-2} yr^{-1})	
Denitrification	71
Manganese reduction	0
Iron reduction	2264
Sulfate reduction	385

[a]Calculated as the sum of the annual DIC and DIN fluxes (mineralization) and C and N burial

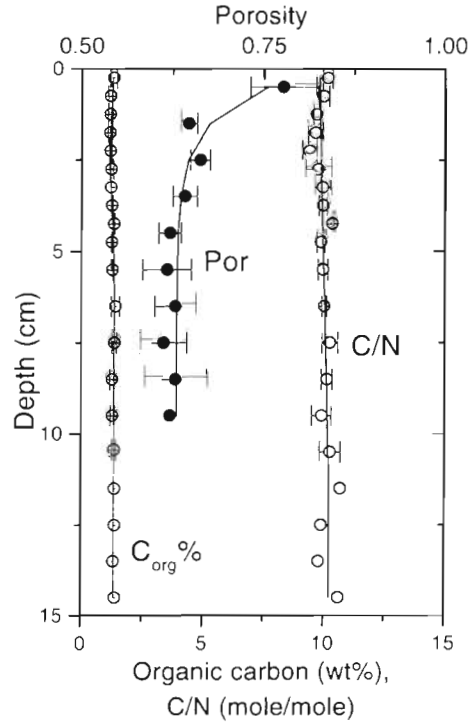

Fig. 3. Depth distribution of porosity, organic carbon (C_{org}), and C:N ratios in the Young Sound sediment. Error bars represent standard error, n = 4

in the surface sediment to 0.62 in 4 cm depth, below which it remained constant (Fig. 3). The organic C content within the sediment varied little with season and was almost constant with depth (1.3 wt %) in the upper 15 cm. Also, the molar ratio of C:N was constant (~10) over the same depth interval (Fig. 3).

Except for oxygen concentration profiles, porewater concentrations of all components measured varied little with season. An example of porewater concentration profiles of O_2, DIC, NH_4^+, NO_3^- + NO_2^-, Mn^{2+}, and Fe^{2+} within the sediment from July 21 is presented in Fig. 4. The O_2 concentration in the overlying water column was always close to atmospheric saturation. Nitrate was measurable down to 1.5 cm with a subsurface maximum of 13 µM at 0.5 cm depth. The DIC concentration increased from 2.2 mM in the overlying water to 3.1 mM at 12 cm depth. The NH_4^+ concentration within the sediment increased from a few µM in the water column to approximately 60 µM at 12 cm depth. The concentrations of Mn^{2+} and Fe^{2+} increased from the surface sediment layer to 25 and 280 µM at 7 and 9 cm depth, respectively. The concentration of SO_4^{2-} was 28 mM in the overlying water and no gradient was detected in the porewater of the upper 15 cm of the sediment (data not shown). Free H_2S was never detected in the porewater (detection limit 1 µM).

Manganese oxides were indicated as a small enrichment of extractable manganese near the surface with a maximum concentration of about twice the stable background level obtained deeper in the sediment (Fig. 4). Subtraction of the background to yield the reactive manganese pool (Aller 1980) showed that reactive manganese was depleted at 2 cm depth. The depth-integrated reactive manganese pool was 14 mmol m^{-2}. Oxalate extractable Fe(III) concentrations were about 2 orders of magnitude higher those of manganese and decreased with depth, although a large amount persisted at 8 to 10 cm (Fig. 4). In parallel to the decrease in Fe(III), which indicated that Fe(III) remaining at this depth was of low activity, the particulate Fe(II) content increased with depth and leveled off at 8 to 10 cm (Fig. 4). Note that decreases in solid components with depth appear less pronounced than increases when concentrations are plotted per cm^3, due to concomitant changes in porosity. Thus, the total extractable iron, Fe(II) + Fe(III), content per g dry weight did not change with depth. Subtraction of this background concentration as for manganese (cf. Thamdrup et al. 1994) demonstrated a reactive Fe(III) pool that decreased in concentration from 45 µmol cm^{-3} at the surface and was not depleted until 8 cm depth. The integrated reactive Fe(III) pool was 1.9 mol m^{-2}, i.e. >100-fold greater than that of reactive manganese.

Most reduced sulfur was found in the chromium reducible pool of FeS_2 and S^0 which increased over the

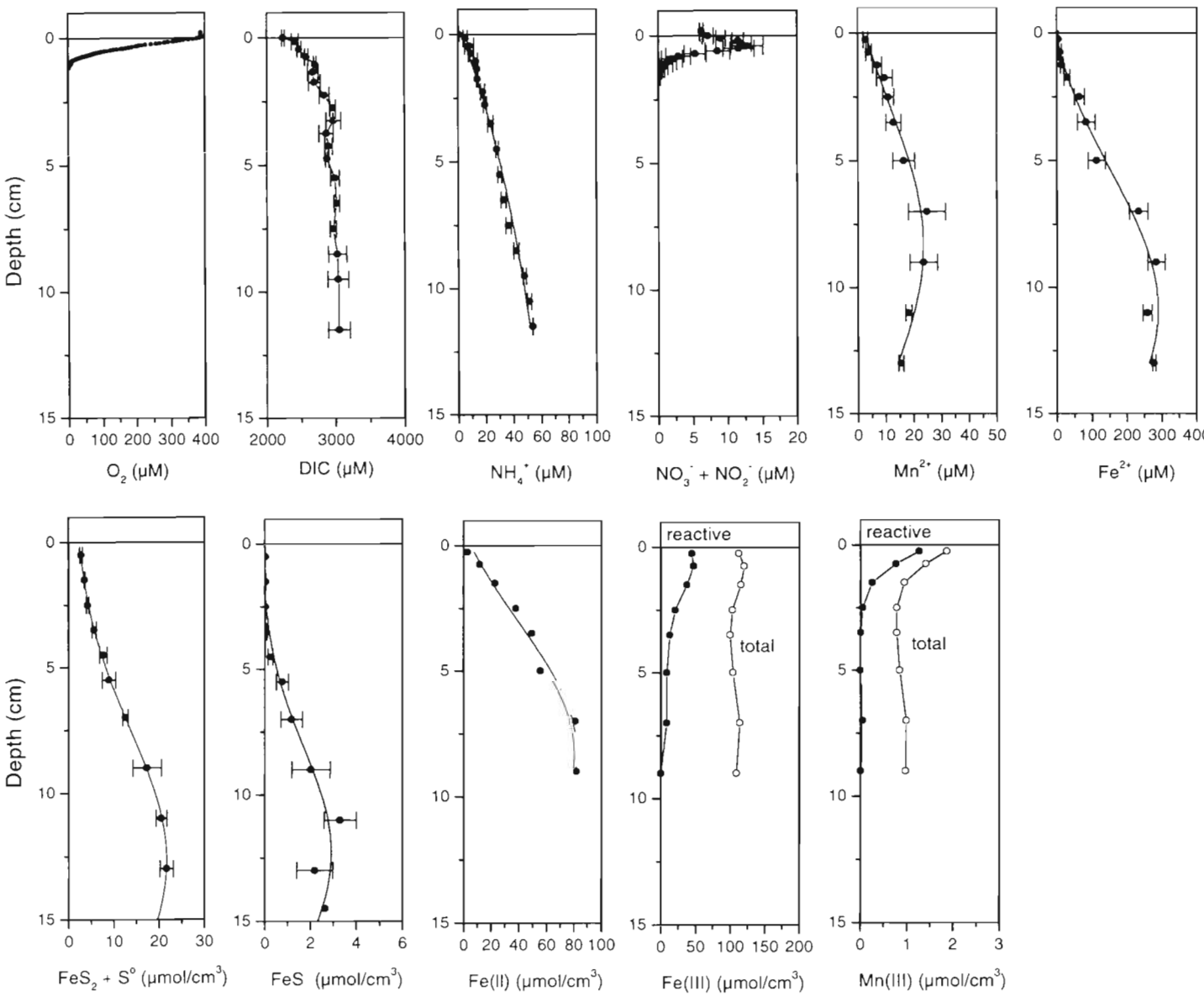

Fig. 4. Porewater concentration profiles of O_2, DIC, NH_4^+, NO_3^- + NO_2^-, Mn^{2+} and Fe^{2+}, as well as the depth distributions of manganese, iron, and sulfur solid species in the sediment of July. Error bars represent standard error, n = 3

entire depth interval and was ~10-fold larger than FeS (Fig. 4). Comparison with pools of Fe(III) and Fe(II) showed that a relatively small fraction of the reactive iron was incorporated into FeS_2 and that FeS contributed insignificantly to particulate Fe(II).

Sediment-water O_2 uptake and nutrient fluxes across the interface

The sediment O_2 uptake increased from a constant level of 5 mmol m^{-2} d^{-1} during sea ice cover to 13 mmol m^{-2} d^{-1} in response to increased bacterial mineralization of fresh organic material settling to the sediment when the sea ice cover broke in July (Fig. 5). A few weeks after the sedimentation peak, the sediment O_2 uptake returned to the basic 5 mmol m^{-2} d^{-1} level due to an effective mineralization of the easily degradable fraction of the settling organic material. The O_2 uptake remained approximately 5 mmol m^{-2} d^{-1} during winter. The opposed fluxes of DIC paralleled the O_2 fluxes (Fig. 5). The O_2:DIC ratio varied with season from 0.9 to 1.3 with an average of 1.0 for the entire year.

The seasonal variation in O_2 fluxes was reflected in the vertical O_2 concentration profiles in the sediment (Fig. 6). The O_2 penetration depth was approximately

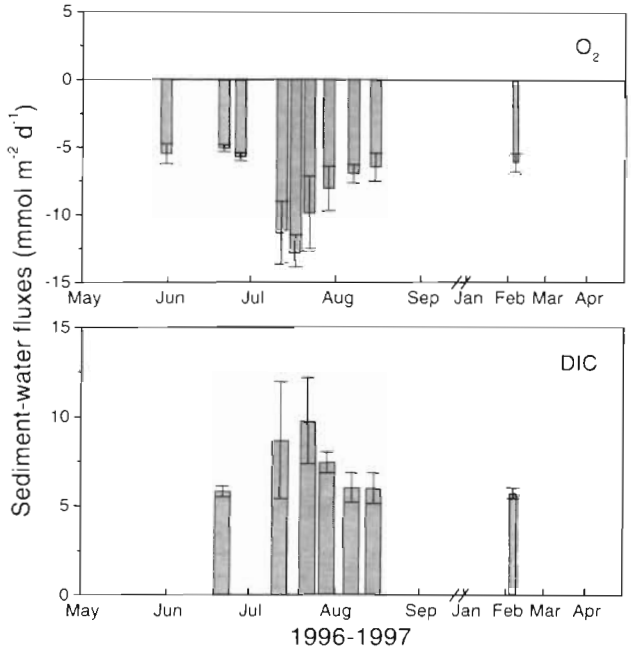

Fig. 5. Seasonal variation in O_2 uptake and DIC release from the sediment of Young Sound. Error bars represent standard error, n = 6. Oxygen fluxes at the end of May are from 1998

1 cm at all sampling dates but the shapes of the concentration profiles were different. Oxygen consumption as a function of depth was calculated using the numerical procedure described by Berg et al. (1998) for interpretation of O_2 concentration profiles (Fig. 6). The highest O_2 consumption rates were found near the sediment-water interface in July, where the input of organic matter to the sediment was enhanced.

The seasonal fluxes of $NO_3^- + NO_2^-$, NH_4^+, urea, PO_4^{3-}, and Si generally showed an increased efflux from the sediment following input of fresh organic material associated with sea ice disappearance (Fig. 7). As in the case of O_2 and DIC fluxes, a constant lower flux was observed during the period with sea ice cover. Nitrate uptake by the sediment was observed in June and in July when sea ice broke. Integrated annual fluxes are summarized in Table 1.

Sediment denitrification rates

The rate of denitrification increased from a steady lower level of approximately 0.2 mmol m^{-2} d^{-1} during sea ice cover to approximately 0.6 mmol m^{-2} d^{-1} following sea ice break-up (Fig. 8). The elevated activity, however, was restricted to a few weeks after ice break-up, after which the activity returned to the basic level. The rate of denitrification was separated into denitrification depending on water column NO_3^- (D_w) and denitrification depending on NO_3^- from nitrification (D_n) (Nielsen 1992). Denitrification was mainly based on NO_3^- being produced by sedimentary nitrification (93% of the total annual denitrification activity, 71 mmol N m^{-2}, Table 1).

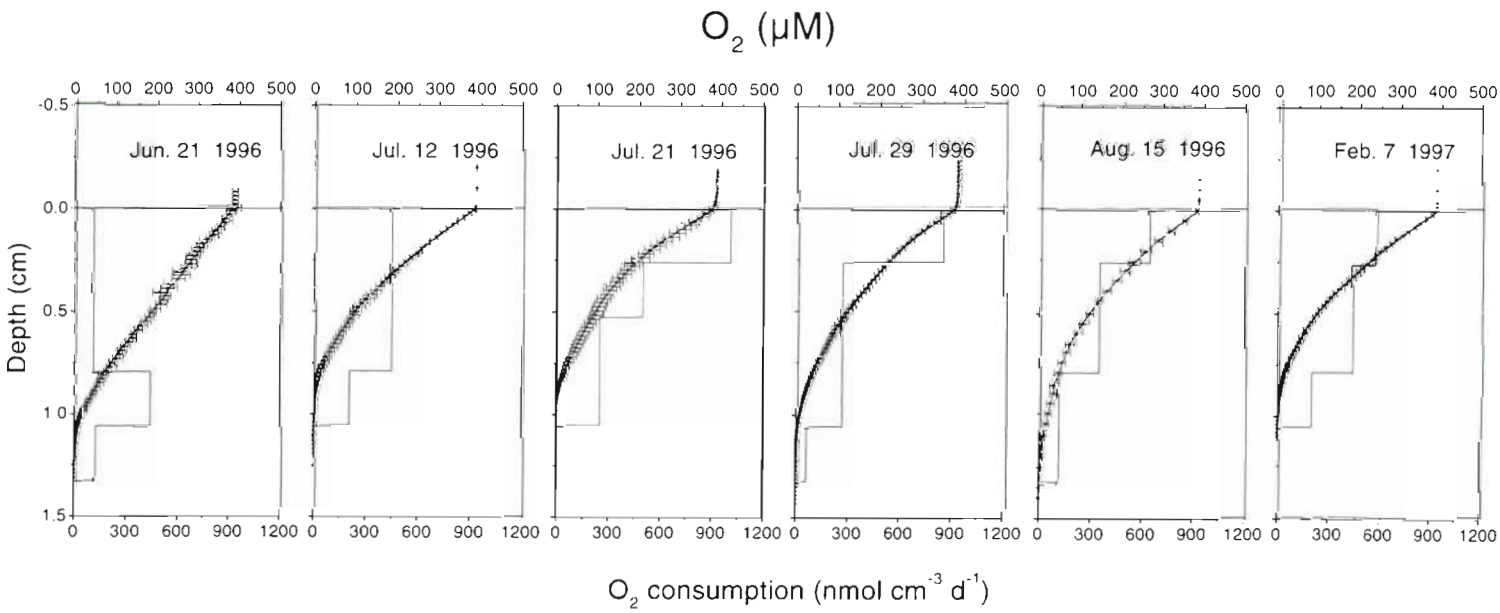

Fig. 6. Seasonal variation in O_2 concentration profiles (dots and lines) and consumption rates (bars) within the sediment of Young Sound. Error bars as in Fig. 5

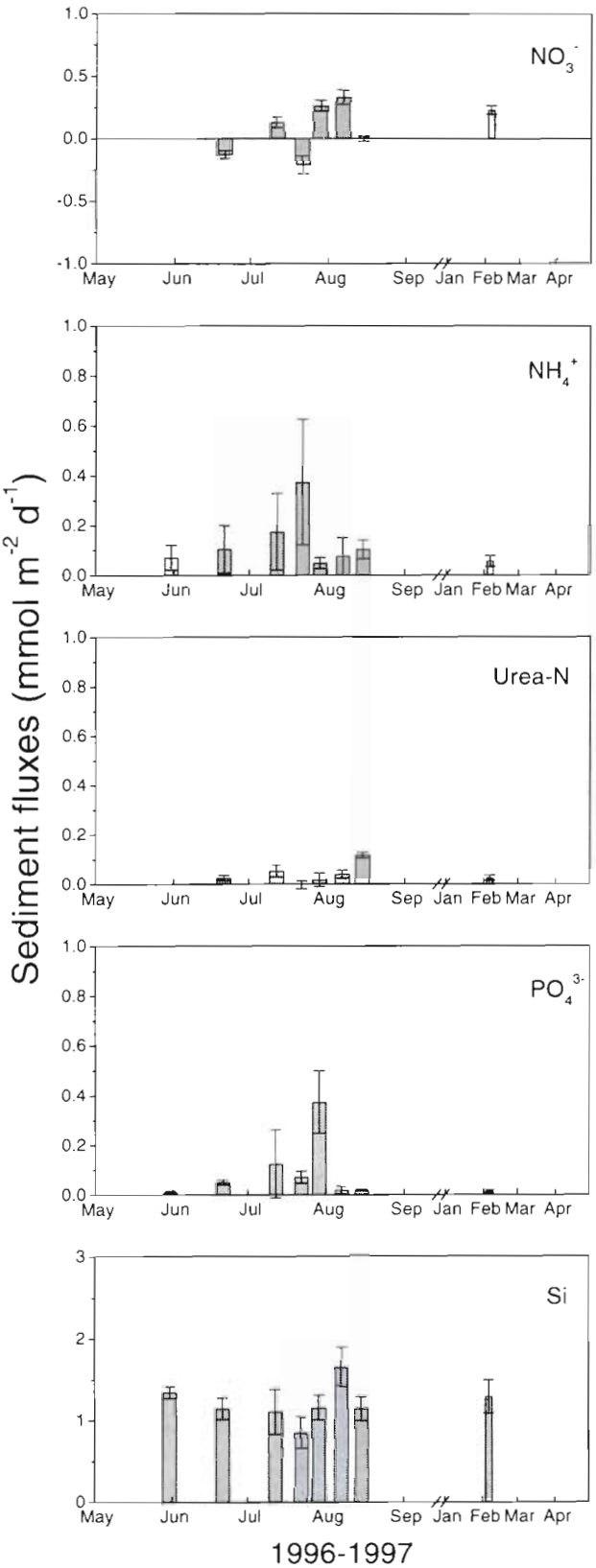

Fig. 7. Seasonal variation in the flux of nutrients in the sediment of Young Sound. Negative values correspond to a sediment uptake. Error bars as in Fig. 5

Sulfate reduction rates

The highest sulfate reduction activities in intact cores were found between 5 and 9 cm depth within the sediment (see Fig. 10). The depth-integrated (0 to 15 cm) sulfate reduction rates were 0.8 to 1.7 mmol m^{-2} d^{-1} with maximum activity occurring immediately after ice break-up and a tendency towards higher rates in the open-water period than during ice cover (Fig. 9). Sulfate reduction rates were not measured during the winter campaign.

Rates and pathways of carbon mineralization (bag incubations)

Porewater concentrations of DIC and NH_4^+ increased linearly during the first 6 d (4 samplings) in all of the 8 depth intervals incubated (r^2 >0.97 for DIC, >0.93 for NH_4^+). In most intervals, the linear increase continued through the remaining 9 d of incubation. Between 1 and 4 cm depth, however, the rates more than doubled during this time. Because of this sudden increase in activity, which was probably due to beginning decay of dead organisms, the rates used in this study were based on the linear increase during the first 6 d of incubation (Fig. 10). Standard errors of the rates were <8% for DIC and <20% for NH_4^+.

The accumulation rates of DIC and NH_4^+ were roughly parallel at all depths. The rates were highest in the surface layer and decreased approximately 5-fold with depth (8 to 10 cm, Fig. 10). Due to adsorption of NH_4^+ to particles (Rosenfeld 1979) the rate of NH_4^+ accumulation in the porewater is an underestimate of the true rate of NH_4^+ production from degradation of organic matter. Assuming an adsorption coefficient of 1.3 for NH_4^+ (Mackin & Aller 1984), we calculated an average C:N mineralization ratio of 7.6 for the bag incubations.

In contrast to DIC and NH_4^+ accumulation rates, sulfate reduction rates reached a maximum at 4 to 6 cm depth (Fig. 10). The zone above this interval was characterized by peaks in the accumulation rates of Mn^{2+} and Fe^{2+} in the porewater, indicating active manganese and iron reduction, although there were no sharp depth separations of the processes. To evaluate the contributions of manganese, iron and sulfate reduction to anoxic mineralization we followed the procedure of Thamdrup & Canfield (1996). The integrated DIC production in the anoxic sediment (1 to 10 cm) was 12.4 mmol m^{-2} d^{-1} and sulfate reduction in the bags was 2.9 mmol m^{-2} d^{-1}, which with a reaction stoichiometry of 1 SO_4^{2-} to 2 organic C corresponded to a DIC production of 5.8 mmol m^{-2} d^{-1} or 47% of the total anaerobic DIC production. The remaining 53% could

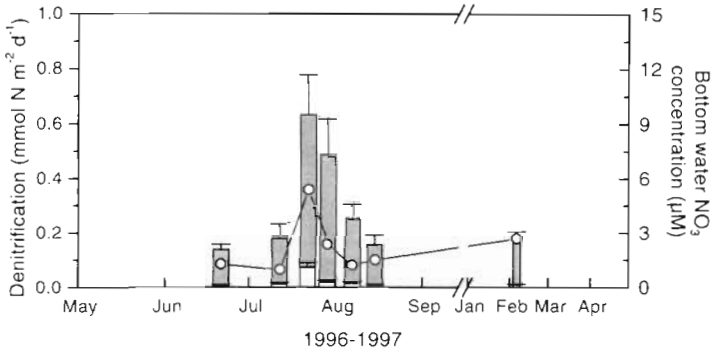

Fig. 8. Seasonal variation in benthic denitrification rates in Young Sound. Open bars: denitrification based on water column NO_3^-; shaded bars: denitrification based on NO_3^- from nitrification. Error bars as in Fig. 5

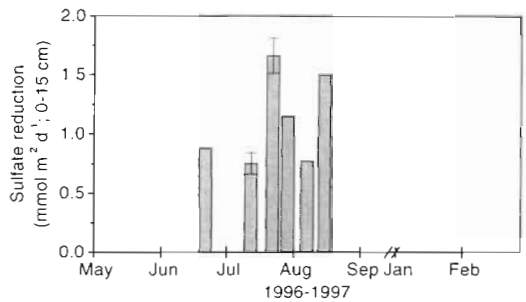

Fig. 9. Seasonal variation in benthic sulfate reduction rates in Young Sound. Error bars represent standard error, n = 3

be attributed to bacterial manganese and iron reduction. Reactive manganese was, however, only detected down to 2 cm (Fig. 4) and only little Mn^{2+} accumulated below this depth (Fig. 10), whereas reactive Fe(III) was available and Fe^{2+} accumulated until 8 cm depth. The 18% of anoxic carbon oxidation that took place at 1 to 2 cm sets an upper limit for the contribution of manganese reduction. However, little reactive manganese was available below 1 cm, and Fe^{2+} accumulated there concomitantly with Mn^{2+}. Thus, all manganese reduction below 1 cm could be coupled to abiotic oxidation of Fe^{2+} (Postma 1985, Canfield et al. 1993a). Based on this analysis, we attribute all the sulfate-independent anoxic carbon oxidation between 1 and 10 cm depth to dissimilatory bacterial iron reduction amounting to 53% of the anaerobic degradation. The absence of both reactive Fe(III) and of Fe^{2+} accumulation below 8 cm depth excluded significant dissimilatory iron reduction at greaterer depths.

Sulfate reduction rates in the bags were about 2.5-fold higher than the rates measured in whole cores during July, and the bag DIC production was 1.6-fold higher than the benthic DIC flux at that time. These differences may suggest that the activity in the bags was stimulated through sediment homogenization, but we do not expect it to have affected the pathways of carbon oxidation differentially. Based on these considerations, we used whole-core sulfate reduction rates as the basis for the calculation of the contribution of iron and sulfate reduction to the annual carbon budget (see 'Discussion').

Burial of carbon and nitrogen within the sediment

The unsupported ^{210}Pb content decreased exponentially with depth. However, surface sediment mixing caused by bioturbation may be apparent in the upper ~4 cm (Fig. 11). The concentration of ^{137}Cs was highest

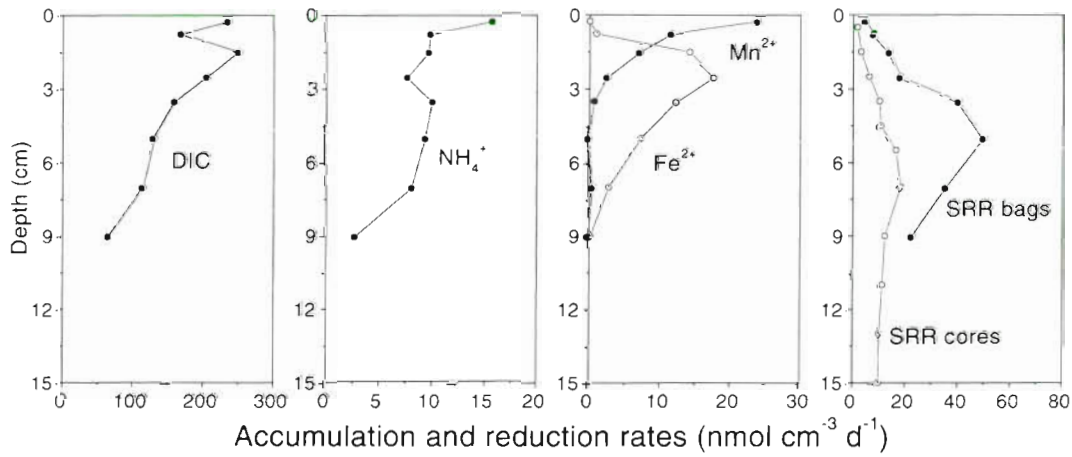

Fig. 10. Accumulation rates of DIC, NH_4^+, Mn^{2+}, Fe^{2-}, and sulfate reduction rates in the sediment of Young Sound as determined from anoxic bag incubations and from intact sediment cores collected at the end of July (see text for further details)

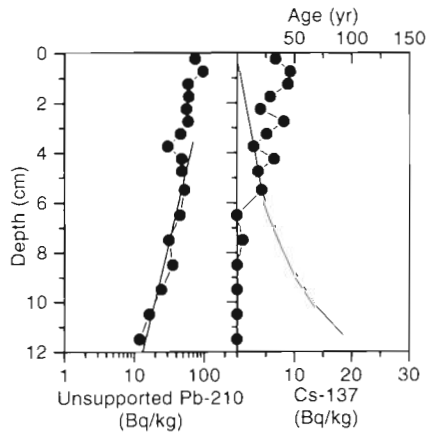

Fig. 11. Depth distribution of unsupported ^{210}Pb and of ^{137}Cs in the sediment of Young Sound. Sediment age illustrated by a line without data points

in the upper 6 cm of the sediment and also decreased with depth. The sediment burial rate calculated on the basis of the profiles was 0.23 cm yr^{-1}.

DISCUSSION

Sedimentation of organic material

The measurements of sedimentation rates made during the summer period in the present study (Table 1) are comparable with measurements from coastal areas in Arctic Canada (Atkinson & Wacasey 1987) during the same time period, but higher than measurements from more open waters in the Greenland Sea (Hebbeln & Wefer 1991, Bauerfeind et al. 1997). The highest sedimentation rates in the above and present study are found during the relatively short and productive open-water period during the few summer months where up to 65% of total annual sedimentation may occur (Atkinson & Wacasey 1987).

Benthic O_2 uptake and nutrient fluxes

The sediment O_2 uptake rates measured in this study (5 to 13 mmol m^{-2} d^{-1}) are within the ranges measured in other Arctic areas: Svalbard (3 to 16 mmol m^{-2} d^{-1}, Pfannkuche & Thiel 1987, Hulth et al. 1994, Glud et al. 1998), Bering and Chukchi Seas (4 to 25 mmol m^{-2} d^{-1}, Grebmeier & McRoy 1989, Henriksen et al. 1993, Devol et al. 1997), and off Newfoundland (8 mmol m^{-2} d^{-1}, Pomeroy et al. 1991).

The O_2 consumption of the sediment showed a distinct seasonal variation. When sea ice broke in July, the increases in sediment O_2 uptake and DIC fluxes were caused by increased bacterial mineralization of settling fresh organic material (Fig. 5). The increased bacterial activity following the input of fresh organic material was also evident from direct measurements of denitrification and, to a lesser extent, sulfate reduction activities (Figs. 8 & 9, respectively). Due to rapid mineralization of the easily degradable fraction of settling organic material, the sediment O_2 uptake and DIC flux returned to the previous lower level only a few weeks after the sedimentation event and remained constant during winter. Subtraction of the mean fluxes measured during ice cover in June and February showed that the summer peak in activity accounted for 270 mmol m^{-2} or 11% of the total annual oxygen flux and a similar fraction of the DIC flux.

Assuming that organic matter reached the sediment in a brief pulse, the exponential decrease in the oxygen uptake during July and August corresponded to a first order decay constant for this labile organic fraction of 19 ± 6 yr^{-1} (r^2 = 0.90). This value is similar to decay constants for fresh phytoplankton determined by others at 20 to 22°C (7 to 26 yr^{-1}; compiled by Westrich & Berner 1984), which indicates that the initial mineralization of organic matter in this permanently cold sediment was highly efficient and exhibited no temperature inhibition.

The seasonal variation in O_2 uptake rates in Young Sound was reflected in the vertical O_2 concentration profiles within the sediment (Fig. 6). Although no major seasonal difference in O_2 penetration into the sediment was observed, the vertical maximum O_2 consumption rates differed between sampling dates. In June, when sea ice covered Young Sound, the maximum O_2 consumption rate was found at 1 cm depth near the oxic-anoxic interface, presumably due to reoxidation of reduced products being transported upwards to the oxic zone. In July, however, following the sea ice break-up and input of organic material to the sediment, the maximum O_2 consumption rate was found in the top layer of the sediment. In August, surface O_2 consumption rates decreased, and the further reduction found in February indicates that input of organic matter was low during winter and that respiration was based on a less easily degradable fraction of the organic material supplied during summer.

In contrast to the O_2 porewater concentration profile, concentration profiles of DIC, NH_4^+, NO_3^- + NO_2^-, Mn^{2+}, Fe^{2+} and SO_4^{2-} did not alter significantly with season. However, profiles of e^--acceptors (O_2, NO_3^-, Fe(III) and SO_4^{2-}) and reduction rate measurements supported the classical orderly progression from O_2 respiration to NO_3^- reduction followed by iron reduction and finally sulfate reduction (Froelich et al. 1979).

The seasonal fluxes of NO_3^- + NO_2^-, NH_4^+, urea, PO_4^{3-}, and Si generally showed an increased efflux

from the sediment following input of fresh organic material associated with sea ice disappearance (Fig. 7). As in the case of O_2 and DIC fluxes, steadily lower fluxes were observed during the period with sea ice cover. The molar DIC:Si:N:P ratio released from the sediment to the overlying water column on an annual basis was 177:34:6:1 Compared with the Redfield ratio (106:15:16:1), nutrient fluxes from the Young Sound sediment suggest that nitrogen may limit primary production as also discussed in a detailed description of phytoplankton nutrient limitation within the Sound (Rysgaard et al. 1999). When N_2 production from denitrification is included into the N flux, the resulting molar ratio of DIC:Si:N:P is 177:34:11:1. The resultant C:N ratio of 16 is higher than the C:N ratio in the settling material from the sediment traps (10 to 12), the C:N ratio of approximately 10 measured in the sediment (Fig. 3), and the C:N mineralization ratio of 7.6 inferred from bag incubations. Thus, although N was mainly mineralized within the sediment, it appears that DIC was preferentially released to the bottom water. However, this difference may in part be explained by the relatively large variation in ammonia fluxes and denitrification rates between replicate cores. Blackburn et al. (1996) reported a similar, although much more pronounced, imbalance from Svalbard sediments, and explained it by non-steady-state assimilation of nitrogen in the sediment. Since the present results cover an annual cycle, this explanation seems less likely here. Alternatively, grazing could constitute an important sink for nitrogen that was missed in the present study.

Denitrification

The increase in denitrification activity was associated with the higher input of organic material to the sediment when the sea ice disappeared during the summer thaw. Liberation of NH_4^+ due to mineralization of organic matter during the summer thaw increased the bacterial nitrification activity and consequently the coupled nitrification-denitrification activity (D_n). Due to a relatively low NO_3^- concentration in the bottom water during all seasons and a deep penetration of O_2 into the sediment, the rate of denitrification based on NO_3^- from the water column was of minor importance in Young Sound, constituting only 7% of the total annual denitrification activity.

The observed total denitrification rates (0.2 to 0.6 mmol N m^{-2}) are within the range reported from other Arctic areas: Svalbard, Norway (0.2 to 0.6 mmol N m^{-2}, Glud et al. 1998); Alaska coastal waters and shelf areas (0.4 to 2.8 mmol N m^{-2}, Henriksen et al. 1993, Devol et al. 1997). Furthermore, these Arctic denitrification rates are comparable with rates from temperate areas with a much higher environmental temperature (Jenkins & Kemp 1984, Nielsen 1992, Rysgaard et al. 1995, Lohse et al. 1996), suggesting that nitrification and denitrification activity is regulated by temperature to a lesser extent than previously assumed.

Manganese, iron, and sulfate reduction rates

The small inventory of reactive manganese oxides excluded a significant contribution to carbon oxidation, and manganese reduction was probably mainly coupled to the reoxidation of reduced iron and sulfur compounds as is the case in typical temperate coastal sediments (e.g. Canfield et al. 1993a, Aller 1994, Thamdrup et al. 1994). Ferric iron, on the other hand, was an important electron acceptor, and the contribution to carbon oxidation was similar to that previously reported from warmer sites (Canfield et al. 1993b, Thamdrup & Canfield 1996). Our results add new width to the thermal range within which significant activity of iron-reducing bacteria has been shown.

Division of the reactive Fe(III) inventory by the rate of iron reduction results in a turnover time for this Fe(III) pool of ~300 d. This is quite slow compared with earlier studies (Canfield et al. 1993a, Thamdrup et al. 1994, Thamdrup & Canfield 1996), but still rapid in comparison with the burial of Fe(III) in the anoxic zone by sediment accumulation. Thus, here as elsewhere, physical reworking of the sediment is essential for the intense iron cycling. Bioturbation was documented both by the presence of an abundant and diverse infauna (Sejr et al. unpubl.) and by the shape of the ^{210}Pb profiles in the upper 4 cm of the sediment (Fig. 11).

In agreement with the high availability of the more favorable oxidants O_2 and reactive Fe(III), sulfate reduction rates attained their maximum relatively deep in the sediment, and the integrated rates were moderate in comparison with rates from both temperate sediments (Skyring 1987, Canfield 1993) and from polar areas (Nedwell et al. 1993).

Burial of carbon and nitrogen within the sediment

The organic matter that escapes oxidation within the sediment by the processes discussed above will become buried and preserved. Assuming that carbon oxidation was restricted to the upper 15 cm of the sediment, as indicated by sulfate reduction profiles in the intact sediment cores, the burial of refractory carbon within the sediment was 2110 mmol m^{-2} yr^{-1} and that of nitrogen 205 mmol N m^{-2} yr^{-1} calculated from the

sediment growth rate and the C and N contents at 10 cm (Figs. 3 & 11, Table 1).

The relatively high ^{137}Cs concentration in the upper 6 cm of the sediment corresponds to the increase in the East Greenland current ^{137}Cs concentrations observed after 1980 due to discharge from the nuclear fuel reprocessing plant Sellafield, UK (Dahlgaard 1994), and to the major fall-out peak from atmospheric nuclear tests centered around 1962–1964 (Aarkrog et al. 1993). It is possible that a significant fraction of the observed ^{137}Cs is caused by long distance transport via the East Greenland current to Young Sound, which indicates that other particle-bound pollutants may also reach this high-Arctic ecosystem.

Annual carbon budget in Young Sound

An annual budget of carbon cycling for the sampling station is presented in Fig. 12. Annual rates were calculated as time-weighted averages. Total annual carbon flux into the sediment was estimated as the sum of the annual DIC flux (2295 mmol C m^{-2}) and carbon burial within the sediment (2110 mmol C m^{-2}) and corresponds to 4405 mmol C m^{-2} (Fig. 12). Thus, 48% of the carbon entering the sediment was preserved through burial, which places Young Sound among average marine sediments with similar sedimentation rates (Canfield 1993), and further substantiates that the low temperature did not inhibit benthic mineralization.

To estimate the relative contributions of the anaerobic processes to total mineralization over the annual cycle, we used the DIC flux as a measure of total carbon mineralization within the sediment. Furthermore, the relative contributions of iron and sulfate reduction to anaerobic mineralization within the sediment (0 to 10 cm) were assumed to remain at 53 and 47%, respectively, throughout the year, as determined in the bag incubations. Sulfate reduction rates from the intact cores were used to calculate the absolute iron reduction rates. Thus, the integrated annual rate of carbon mineralization due to sulfate reduction in the 0 to 10 cm interval investigated in bag incubations, 502 mmol C m^{-2}, yielded a contribution from iron reduction of 566 mmol C m^{-2} (502 × 53/47). The contribution from sulfate reduction, integrated to 15 cm, was 769 mmol C m^{-2} yr^{-1}, and denitrification mineralized 89 mmol C m^{-2} yr^{-1}. Considering the upper 15 cm of the sediment, these figures correspond to contributions of 4, 25, and 33% from denitrification, iron reduction, and sulfate reduction, respectively, leaving 871 mmol C yr^{-1} or 38% of carbon oxidation to organotrophic

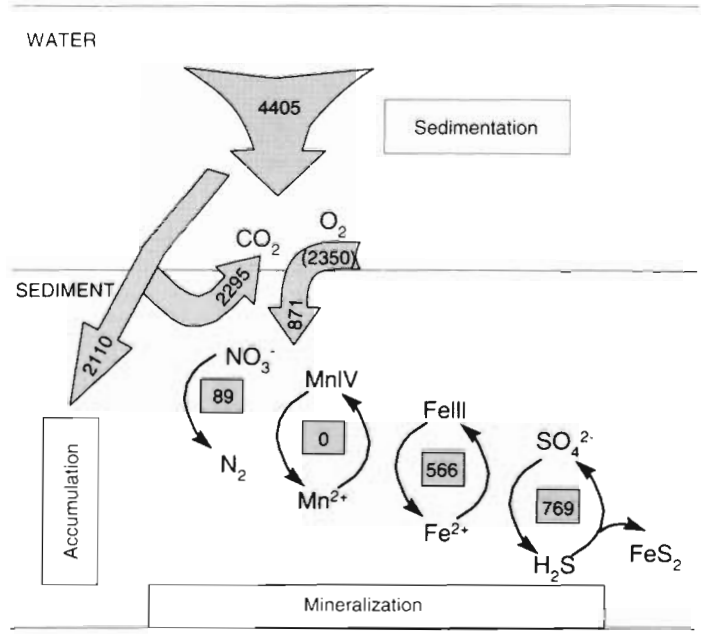

Fig. 12. Annual carbon budget for the investigated station in Young Sound (36 m). All units are in mmol C m^{-2} yr^{-1} except for the O_2 consumption rate (in brackets), which is in mmol O_2 m^{-2} yr^{-1}. See text for further explanation

oxygen respiration (Fig. 13). The difference between the measured sediment-water O_2 uptake rate (2350 mmol O_2 m^{-2} yr^{-1}) and the direct carbon oxidation by oxygen respiration (871 mmol C m^{-2} yr^{-1}) represents 63% of the O_2 uptake which was used to re-oxidize reduced components from anaerobic mineralization.

The contribution of O_2 respiration to total carbon oxidation in Young Sound sediment was intermediate

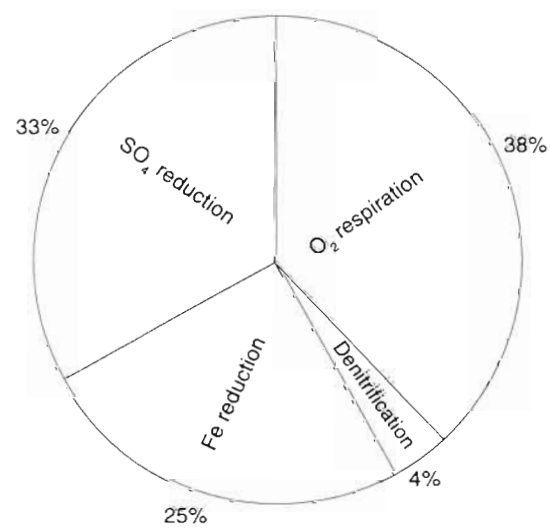

Fig. 13. Importance of different carbon oxidation pathways in Young Sound

compared with recent results from Aarhus Bay (Jørgensen 1996) and from Chile (Thamdrup & Canfield 1996) and the Skagerrak (Canfield et al. 1993b). A general trend in all studies, however, was that denitrification accounted for a relatively small fraction of total carbon oxidation, whereas iron and sulfate reduction played an important part. Furthermore, the relatively high contribution of iron reduction to total mineralization in Young Sound adds to the small database that supports the general importance of iron reduction in sedimentary carbon oxidation. If iron reduction had been ignored, we would have found a contribution of anaerobic mineralization of only 37%, similar to the 32% calculated for an Antarctic site, where iron reduction was not taken into account (Nedwell et al. 1993). Thus, inclusion of iron reduction shifts the balance between aerobic and anaerobic mineralization significantly.

Data from Young Sound indicate that the contribution of O_2 respiration to total carbon oxidation may not be constant over the year since a decrease in the relative importance of aerobic mineralization was observed following input of organic material when the sea ice broke (data not shown). As shown in other investigations, large increases in organic additions to sediments decrease the O_2 penetration depth and consequently narrow the oxic zone where carbon oxidation by O_2 respiration can proceed (Rasmussen & Jørgensen 1992, Caffrey et al. 1993). Therefore, the relative contribution of O_2 respiration to total carbon oxidation will be expected to decrease with increasing organic loading while the anaerobic processes manganese, iron, and sulfate reduction will increasingly dominate mineralization.

Conclusion

On an annual basis, aerobic and anaerobic mineralization contributed 38 and 62%, respectively, of the degradation of organic matter in this Arctic sediment. Furthermore, it was observed that bacterial iron reduction accounted for a significant fraction of anaerobic mineralization. Approximately half of the organic carbon reaching the sediment was permanently buried due to incomplete degradation. The increased bacterial mineralization associated with the sea ice break-up during the summer thaw resulted in a rapid increase in efflux of nutrients to the water column, revealing an efficient coupling between production in the water column and degradation within the sediment. Thus, the observation that seasonal variation in benthic mineralization and consequently fluxes responded to increased input of organic material following sea ice disappearance indicates that benthic mineralization within this Arctic coastal sediment was regulated by the availability of organic matter and not by seasonal bottom water temperature, which was constant. Furthermore, bacterial activities were comparable with bacterial activities in sediments with a much higher ambient temperature. These findings support conclusions from other recent studies from Arctic (Rysgaard et al. 1996, Glud et al. 1998) as well as Antarctic (Nedwell et al. 1993) areas and contradict the assumption that microbial decomposition is generally low in cold waters (Pomeroy & Deibel 1986).

Acknowledgements. This study was financially supported by the Danish Research Councils (contract no. 9501025 and 9700224), The European Union under the framework of MAST III (Marine Science and Technology III) and ELOISE (European Land-Ocean Interaction Studies) contract # MAS3-CT96-0048 and by the Max Planck Society. The Danish Polar Center is acknowledged for logistic support. The Danish Military Division, Sirius, is thanked for its hospitality. Egon Frandsen, Marlene Jessen, Kitte Gerlich and Anna Haxen are thanked for technical assistance in the field or laboratory. Ronni N. Glud, Ola Holby and N. P. Revsbech are thanked for helpful discussions and help in the field. Lars H. Larsen is acknowledged for the analysis of nitrate porewater concentrations. Finally, Anna Haxen is thanked for linguistic corrections.

LITERATURE CITED

Aarkrog A, Dahlgaard H, Hallstadius L, Hansen H, Holm E (1993) Radiocaesium from Sellafield effluents in Greenland waters. Nature 304:49–51

Aller RC (1980) Diagenetic processes near the sediment-water interface of Long Island Sound. 2. Fe and Mn. Adv Geophys 22:351–415

Aller RC (1994) The sedimentary Mn cycle in Long Island Sound: its role as intermediate oxidant and the influence of bioturbation, O_2, and C_{org} flux on diagenetic reaction balances. J Mar Res 52:259–295

Atkinson EG, Wacasey JW (1987) Sedimentation in Arctic Canada: particulate organic carbon flux to a shallow marine benthic community in Frobisher Bay. Polar Biol 8: 3–7

Bauerfeind E, Garrity C, Krumbholz M, Ramseier RO, Voss M (1997) Seasonal variability of sediment trap collections in the Northeast Water Polynia. Part 2. Biochemical and microscopic composition of sedimenting matter. J Mar Syst 10:371–389

Berg P, Risgaard-Petersen N, Rysgaard S (1998) Interpretation of measured concentration profiles in sediment pore water. Limnol Oceanogr 6:1500–1510

Blackburn TH, Hall POJ, Hulth S, Landén A (1996) Organic-N loss by efflux and burial associated with a low efflux of organic N with nitrate assimilation in Arctic sediments (Svalbard, Norway). Mar Ecol Prog Ser 141:283–293

Bower C, Holm-Hansen T (1980) A salicylate-hypochlorite method for determining ammonia in seawater. Can J Fish Aquat Sci 37:794–798

Caffrey JM, Sloth NP, Kaspar HF, Blackburn TH (1993) Effect of organic loading on nitrification and denitrification in a marine sediment microcosm. FEMS Microbiol Ecol 12: 159–167

Canfield DE (1993) Organic matter oxidation in marine sediments. In: Wollast R, Mackenzie, FT, Chou L (eds) Interaction of C, N, P and S biogeochemical cycles and global change. NATO Series, Vol 14. Springer-Verlag, Berlin, p 333–363

Canfield DE, Thamdrup B, Hansen JW (1993a) The anaerobic degradation of organic matter in Danish coastal sediments: Fe reduction, Mn reduction and sulfate reduction. Geochim Cosmochim Acta 57:2563–2570

Canfield DE, Jørgensen BB, Fossing H, Glud R, Gundersen J, Ramsing NB, Thamdrup B, Hansen JW, Nielsen LP, Hall POJ (1993b) Pathways of organic carbon oxidation in three continental margin sediments. Mar Geol 113:27–40

Christensen E (1982) A model for radionuclides in sediments influenced by mixing and compaction. J Geophys Res 87: 566–572

Cline JD (1969) Spectrophotometric determination of hydrogen sulfide in natural waters. Limnol Oceanogr 14: 454–458

Dahlgaard H (1994) Sources of ^{137}Cs, ^{90}Sr and ^{99}Tc in the East Greenland current. J Environ Radioactivity 25:37–55

Devol AH, Codispoti LA, Christensen JP (1997) Summer and winter denitrification rates in western Arctic shelf sediments. Cont Shelf Res 17:1029–1050

Fossing H, Jørgensen BB (1989) Measurement of bacterial sulfate reduction in sediments: evaluation of a single-step chromium reduction method. Biogeochemistry 8:205–222

Froelich PN, Klinkhammer GP, Bender ML, Luedtke GR, Heath GR, Cullen D, Dauphin P (1979) Early oxidation of organic matter in pelagic sediments of the eastern equatorial Atlantic: suboxic diagenesis. Geochim Cosmochim Acta 43:1075–1090

Glud RN, Holby O, Hoffmann F, Canfield D (1998) Benthic mineralization and exchange in Arctic sediments (Svalbard). Mar Ecol Prog Ser 173:237–251

Grasshoff K, Erhardt M, Kremling K (1983) Methods of seawater analysis, 2nd edn. Verlag Chemie, Weinheim

Grebmeier JM, McRoy CP (1989) Pelagic-benthic coupling on the shelf of the northern Bering and Chukchi Seas. III. Benthic food supply and carbon cycling. Mar Ecol Prog Ser 53:79–91

Hall POJ, Aller RC (1992) Rapid, small-volume, flow injection for analysis for total CO_2 and NH_4^+ in marine and freshwaters. Limnol Oceanogr 37:1113–1119

Hansen J (1992) Den økologiske betydning af mangan i marine sedimenter herunder oxidation af reducrerde svovlforbindelser. MS thesis, Univ Århus

Hebbeln D, Wefer G (1991) Effects of ice coverage and ice-rafted material on sedimentation in the Fram Strait. Nature 350:409–411

Henriksen K, Blackburn TH, Lomstein BAa, McRoy CP (1993) Rates of nitrification, distribution of nitrifying bacteria and inorganic N fluxes in northern Bering-Chukchi shelf sediments. Cont Shelf Res 13:629–651

Hulth S, Blackburn TH, Hall POJ (1994) Arctic sediments (Svalbard): consumption and microdistribution of oxygen. Mar Chem 46:293–316

Jenkins MC, Kemp WM (1984) The coupling of nitrification and denitrification in two estuarine sediments. Limnol Oceanogr 29:609–619

Jørgensen BB (1978) A comparison of methods for the quantification of bacterial sulfate reduction in coastal marine sediments. I. Measurement with radiotracer techniques. Geomicrobiol J 1:11–27

Jørgensen BB (1996) Case study—Aarhus Bay. In: Jørgensen BB, Richardson K (eds) Eutrophication in coastal and marine ecosystems, Series IV, American Geophysical Union, Washington, DC

Joshi SR (1987) Nondestructive determination of lead-210 and radium-226 sediments by direct photon analysis. J Radioanalyt Nucl Chem Art 116:169–182

Kelly JR, Nixon SW (1984) Experimental studies of the effect of organic deposition on the metabolism of a coastal marine bottom community. Mar Ecol Prog Ser 17:157–169

Kruse B (1993) Measurement of plankton O_2 respiration in gas-tight plastic bags. Mar Ecol Prog Ser 94:155–163

Larsen LH, Kjær T, Revsbech NP (1997) A microscale NO_3^- biosensor for environmental applications. Anal Chem 69: 3527–3531

Lohse L, Kloosterhuis T, van Raaphorst W, Helder W (1996) Denitrification rates as measured by the isotope pairing method and by the acetylene inhibition technique in continental shelf sediments of the North Sea. Mar Ecol Prog Ser 132:169–179

Lord CJ (1980) The chemistry and cycling of iron, manganese, and sulfur in salt marsh sediments. PhD thesis, University of Delaware, Lewes

Mackin JE, Aller R (1984) Ammonium adsorption in marine sediments. Limnol Oceanogr 29:250–257

Nedwell DB, Walker TR, Ellis-Evans JC, Clarke A (1993) Measurements of seasonal rates and annual budgets of organic carbon fluxes in an antarctic coastal environment at Signy Island, South Orkney Islands, suggest a broad balance between production and decomposition. Appl Environ Microbiol 59:3989–3995

Nielsen LP (1992) Denitrification in sediment determined from nitrogen isotope pairing. FEMS Microb Ecol 86: 357–362

Pamatmat MM (1973) Benthic community metabolism on the continental terrace and the deep sea in the North Pacific. Int Rev Ges Hydrobiol 58:345–368

Pfannkuche O, Thiel H (1987) Meiobenthic stocks and benthic activity on the NE-Svalbard Shelf and in the Nansen Basin. Polar Biol 7:253–266

Pomeroy LR, Deibel D (1986) Temperature regulation of bacterial activity during the spring bloom in Newfoundland coastal waters. Science 233:359–361

Pomeroy LR, Wiebe WJ, Deibel D, Thompson RJ, Rowe GT, Pakulski JD (1991) Bacterial responses to temperature and substrate concentration during the Newfoundland spring bloom. Mar Ecol Prog Ser 75:143–159

Postma D (1985) Concentration of Mn and separation from Fe in sediments—1 Kinetics and stoichiometry of the reaction between birnessite and dissolved Fe(II) at 10°C. Geochim Cosmochim Acta 49:1023–1033

Price NM, Harrison PJ (1987) Comparison of methods for the analysis of dissolved urea in seawater. Mar Biol 94: 307–317

Rasmussen H, Jørgensen BB (1992) Microelectrode studies of seasonal oxygen uptake in a coastal sediment: role of molecular diffusion. Mar Ecol Prog Ser 81:289–303

Reeburgh WS (1967) An improved interstitial water sampler. Limnol Oceanogr 12:163–165

Revsbech NP (1989) An oxygen microelectrode with a guard cathode. Limnol Oceanogr 34:474–478

Risgaard-Petersen N, Rysgaard S (1995) Nitrate reduction in sediments and waterlogged soil measured by ^{15}N techniques. In: Alef K, Nannipieri P (eds) Methods in applied soil and microbiology. Academic Press, London, p 287–295

Risgaard-Petersen N, Rysgaard S, Revsbech NP (1993) A sensitive assay for determination of $^{14}N/^{15}N$ isotope distribution in NO_3^-. J Microbiol Meth 17:155–164

Rosenfeld JK (1979) Ammonium adsorption in nearshore anoxic sediments. Limnol Oceanogr 24:356–364

Rysgaard S, Christensen PB, Nielsen LP (1995) Seasonal variation in nitrification and denitrification in estuarine sediment colonized by benthic microalgae and bioturbating infauna. Mar Ecol Prog Ser 126:111–121

Rysgaard S, Finster K, Dahlgaard H (1996) Primary production, nutrient dynamics and mineralization in a northeastern Greenland fjord during the summer thaw. Polar Biol 16:497–506

Rysgaard S, Nielsen TG, Hansen B (1999) Seasonal variation in nutrients, pelagic primary production and grazing in a high-Arctic coastal marine ecosystem, Young Sound, Northeast Greenland. Mar Ecol Prog Ser (in press)

Shiah FK (1994) Temparature and substrate regulation of bacterial abundance, production and specific growth rate in Chesapeake Bay, USA. Mar Ecol Prog Ser 103:297–308

Skyring GW (1987) Sulfate reduction in coastal ecosystems. Geomicrobiol J 5:295–374

Stookey LL (1970) Ferrozine—a new spectrophotometric reagent for iron. Anal Chem 42:779–781

Tahey TM, Duinveld GCA, Berghuis EM, Helder W (1994) Relation between sediment-water fluxes of oxygen and silicate and faunal abundance at continental shelf, slope and deep-water stations in the northwest Mediterranean. Mar Ecol Prog Ser 104:119–130

Thamdrup B, Canfield DE (1996) Pathways of carbon oxidation in continental margin sediments off central Chile. Limnol Oceanogr 41:1629–1650

Thamdrup B, Fossing H, Jørgensen BB (1994) Manganese, iron, and sulfur cycling in a coastal marine sediment, Aarhus Bay, Denmark. Geochim Cosmochim Acta 58: 5115–5129

Thamdrup B, Canfield DE, Ferdelman G, Glud RN, Gundersen JK (1996) A biogeochemical survey of the anoxic basin Golfo Dulce, Costa Rica. Rev Biol Trop 44:19–33

Thamdrup B, Hansen J, Jørgensen BB (1998) Temperature dependence of aerobic respiration in a coastal sediment. FEMS Microb Ecol 25:189–200

Wadhams P (1981) The ice cover in the Greenland and Norwegian seas. Rev Geophys Space Phys 19:345–393

Westrich JT, Berner RA (1984) The role of sedimentary organic matter in bacterial sulfate reduction: the G model tested. Limnol Oceanogr 29:236–249

Editorial responsibility: Otto Kinne (Editor), Oldendorf/Luhe, Germany

Submitted: June 3, 1998; Accepted: September 16, 1998
Proofs received from author(s): November 26, 1998